ELSEVIER

Earth and Planetary Science Letters 184 (2001) 671–683

EPSL

www.elsevier.com/locate/epsl

Constraints on origin and evolution of Red Sea brines from helium and argon isotopes

Gisela Winckler [a,*], Werner Aeschbach-Hertig [b], Rolf Kipfer [b,c], Reiner Botz [d], André P. Rübel [a], Reinhold Bayer [a], Peter Stoffers [d]

[a] *Institute of Environmental Physics, University of Heidelberg, Im Neuenheimer Feld 229, 69120 Heidelberg, Germany*
[b] *Department of Water Resources and Drinking Water, Swiss Federal Institute of Environmental Science and Technology, EAWAG, CH-8600 Dübendorf, Switzerland*
[c] *Isotope Geology, Swiss Federal Institute of Technology, ETH, CH-8092 Zürich, Switzerland*
[d] *Institut für Geowissenschaften, Universität Kiel, Olshausenstrasse 40–60, 24098 Kiel, Germany*

Received 7 June 2000; accepted 6 November 2000

Abstract

Brines from three depressions along the axis of the Red Sea, the Atlantis II, the Discovery and the Kebrit Deep, were sampled and analyzed for helium and argon isotopes. We identified two principally different geochemical fingerprints that reflect the geological setting of the deeps. The Atlantis II and the Discovery brines originating from locations in the central Red Sea show ^{4}He concentrations up to 1.2×10^{-5} cm^3 STP g^{-1} and a ^{3}He/^{4}He ratio of 1.27×10^{-5}. The MORB-like ^{3}He/^{4}He ratio is typical of an active hydrothermal vent system and clearly indicates a mantle origin of the helium component within the brines. ^{40}Ar/^{36}Ar ratios are as high as 305 implying that mantle-derived ^{40}Ar excesses of up to 3% of the total argon concentration are present in the brines and transported along with the mantle helium signal. The mean $(^4\mathrm{He}/^{40}\mathrm{Ar})_{\mathrm{excess}}$ ratio of 2.1 is in agreement with the theoretical mantle production ratio. In the Kebrit Deep, located in the northern Red Sea, we found a helium excess of 5.7×10^{-7} cm^3 STP g^{-1}. The low ^{3}He/^{4}He ratio of 1×10^{-6} points to a predominantly radiogenic source of the helium excess with only a minor mantle contribution of approximately 9%. We propose a new scenario assuming that the Kebrit brine accumulates a diffusive helium flux that migrates from deeper sedimentary or crustal horizons. In contrast to the Atlantis II and Discovery Deep, the Kebrit brine shows no sign of an active hydrothermal input.

Keywords: noble gases; He-3; He-4; Ar-40; hydrothermal vents; brines; mid-ocean ridges; Red Sea

1. Introduction

The Red Sea rift system is an example of a young ocean basin that formed as a result of the break-up of a continent [1,2]. It can be divided into three sections, each representing successive phases of the transition from continental to oceanic rifting [3]. The southern Red Sea is a young spreading center which has developed through normal seafloor spreading during the last 4–5 million years. The central region between 20° and 23°20′ N is interpreted as a transition zone presently changing from diffusive extension to an ac-

* Corresponding author. Tel.: +49-6221-546336; Fax: +49-6221-546405;
E-mail: gisela.winckler@iup.uni-heidelberg.de

0012-821X/01/$ – see front matter
PII: S0012-821X(00)00345-9

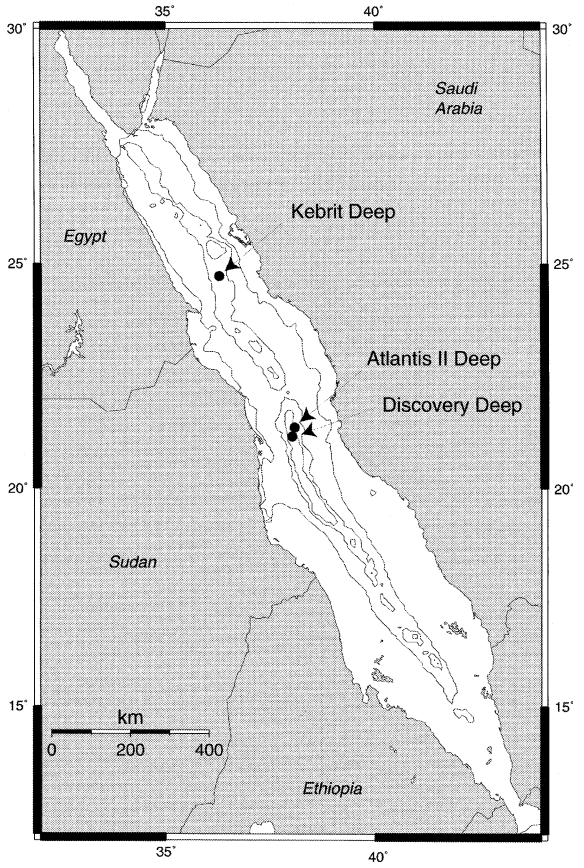

Fig. 1. Map of the Red Sea showing the locations of the three investigated deeps. The Atlantis II Deep (21°22.5′ N, 38°4.5′ E) is the largest brine pool (5×14 km) and is associated with metalliferous sediments of potential economic importance. The Discovery Deep (21°17′ N, 38°3.2′ E) belongs to the Atlantis II Deep area and is situated 5 km southwest of the Atlantis II Deep. The Kebrit Deep belongs to a series of smaller brine pools in the northern Red Sea and is located at 24°43.35′ N, 36°16.6′ E.

tive spreading mode of plate separation. The northern segment represents the pre-seafloor spreading stage in the development of the continental margin [4].

A characteristic feature of the central and northern Red Sea, discovered in 1966, are isolated topographic depressions which are filled with geothermal brines, i.e. waters characterized by elevated salinities and temperatures (e.g. [5–7]). The high salinities are caused by leaching of the Miocene evaporites that underlie the entire Red Sea [8]. The brines occur in one or more horizontally uniform layers, separated by thin interfaces with sharp gradients of temperature and salinity (e.g. [9–11]).

In 1997, the Atlantis II and the Discovery deeps in the central Red Sea and the Kebrit Deep in the northern Red Sea were revisited (Fig. 1). The Atlantis II Deep is the largest and best studied brine pool within this unique geological environment. Isotope investigations have demonstrated that the Atlantis II brine is part of an active hydrothermal system (e.g. [12–14]) but, in spite of numerous studies, there is still considerable debate concerning the detailed origin (e.g. [15,16]) and the dynamics of the brine system [10]. Origin and formation processes of the northern brine pools are still poorly understood.

One of the keys to defining the origin of fluids is application of isotope geochemistry, including helium isotopes. Helium is one of the most sensitive and indicative geochemical tracers for such studies as it is chemically inert and has distinct isotopic signatures in the individual geological reservoirs. In general, helium dissolved in seawater is mainly derived from the atmosphere and characterized by the atmospheric isotope ratio ($R_a = (^3He/^4He)_a = 1.384 \times 10^{-6}$ [17]). The sources of helium in excess of solubility equilibrium with the atmosphere can be identified and quantified by their specific isotopic signatures. So-called radiogenic helium with low $^3He/^4He$ ratios ($1–3 \times 10^{-8}$ [18]) is characteristic for crustal or sedimentary reservoirs where radiogenic ^4He is produced from radioactive decay of uranium and thorium chain elements and accompanied by a small ^3He component of nucleogenic origin. Mantle helium ($^3He/^4He = 1–4 \times 10^{-5}$) is the remnant of the primordial helium inventory trapped in the Earth's mantle at its accretion [19]. Another useful tracer of mantle processes is mantle-derived radiogenic ^{40}Ar produced by the decay of ^{40}K (e.g. [20]). Vent fluids from mid-ocean ridge hydrothermal systems extract the mantle volatiles during hydrothermal circulation through newly formed oceanic crust (e.g. [21]). However, in contrast to the extensive data set for helium isotopes, there exist only very few studies dealing with ar-

gon isotope anomalies in hydrothermal fluids [22,23].

We present a new, detailed set of helium and argon isotope data from three different deeps in order to complement our recent study on atmospheric heavier noble gases [16]. We used a newly developed in situ sampling technique which preserves the undisturbed gas composition of the brine without the disturbing effects of degassing often encountered in sampling extreme marine environments [16]. Major goals of the present study are: (1) to identify the geochemical signatures of the different brine systems, (2) to develop a formation scenario for the Kebrit Deep in the northern Red Sea, potentially representative for other brine pools in the northern Red Sea, (3) to re-evaluate the proposed origin of the Atlantis II system, and (4) to compare the formation processes of the Kebrit and the Atlantis II brines in relation to their geological settings.

2. Methods

Water samples for noble gas analysis were obtained during cruise 121 of RV *Sonne* in 1997. One set of the samples (later referred to as Niskin samples, N) was taken using the standard procedure for helium sampling, i.e. on-board transfer of the water from the Niskin bottle to copper tubes immediately after recovery of the rosette. As this standard sampling procedure is known to be problematic for extreme marine environments with high dissolved gas concentrations (mainly CH_4 and CO_2, e.g. [26]) we obtained a second set of samples using a new in situ sampling technique developed at the ETH Zürich [16]. This device seals the samples in copper tubes under in situ conditions and thus avoids degassing losses owing to pressure release on the up-cast and during the water transfer from the Niskin bottle to the copper tube. Thus, the in situ samples (referred to as Q) represent the 'original' brine composition as has been shown in [16].

2.1. Analytical procedures

The helium isotopes of the Niskin samples were measured at the Institute of Environmental Physics at the University of Heidelberg using a VG MM 3000 sector field mass spectrometer [24]. The in situ samples were analyzed for all noble gases and their isotopic composition at the noble gas laboratory at ETH Zürich [25]. The heavier noble gas data have been discussed elsewhere [16].

2.2. Data evaluation

Comparison between the duplicates (four samples were taken by both sampling procedures) allows us to evaluate potential degassing effects occurring during Niskin sampling. Large differences of the composition between Niskin and in situ samples were observed in the brine layers of the Atlantis II brine, where the CH_4 concentrations are of the order of 100 μl l^{-1} and higher, and in the Kebrit brine which shows extremely high methane concentrations up to 22 ml l^{-1} [26]. Such high amounts of hydrocarbons and CO_2 may degas and form bubbles as the Niskin bottle is raised through the water column and the partial pressure of the dissolved gases exceeds the hydrostatic pressure. The CH_4 bubbles are initially free of noble gases and may strip gases from the water. Consequently, the Niskin samples do not deliver representative concentration data: if the bubbles are not included in the sampler, the gas concentrations are depleted, and if the bubbles are preferentially included in the sample, the gas concentrations are overestimated. In any case, for waters with CH_4 concentrations > 20 μl l^{-1}, i.e. all brine layers of the Atlantis II Deep and the Kebrit Deep, we do not consider the Niskin samples for data evaluation but only the in situ samples. Niskin samples from layers with lower CH_4 concentrations < 20 μl l^{-1} (Discovery Deep and transition zones) are not affected by degassing processes which is demonstrated by the very good agreement of the results of one duplicate from the Discovery Deep (see Table 1, N31, Q357). Our results show that tracer studies in extreme marine environments with high gas concentrations require an in situ sampling method such as the ETH sampler used in this study.

3. Results

3.1. Atlantis II and Discovery deeps

The Atlantis II Deep contains the brine with the highest known temperature (67.2°C) and salinity (260‰) within the Red Sea. It is characterized by four brine layers, the lower convective layer (LCL) and the upper convective layers UCL1, UCL2 and UCL3, and an overlying transition zone. We obtained 10 Niskin samples in and above the transition zone and five in situ samples in the brine layers LCL, UCL1 and UCL3 (see Table 1 and Fig. 2).

The Discovery Deep contains a single 45.1°C brine layer, LCL, which is overlaid by a 150 m thick transition zone (see temperature distribution in Fig. 2). In the Discovery Deep, we collected

Table 1
Helium isotope signature of the Atlantis II, Discovery and Kebrit deeps

Layer	Number	Depth (m)	$^3He/^4He$ (10^{-6})	^4He (10^{-8} cm^3 STP g^{-1} $_{RSDW}$)	Salinity[a] (‰)	Temperature[a] (°C)
Atlantis II Deep						
Trans	N12	1914	9.690	15.3	41	22.9
Trans	N35	1924	9.710	16.3	42	23.5
Trans	N18	1925	9.690	16.5	51	23.3
Trans	N36	1956	10.4	22.3	44	24.3
UCL3	Q407	2005	12.68	315	90	45.1
UCL1	Q261	2024	12.66	662	147	56.4
UCL1	Q67	2042	12.74	655	147	56.4
LCL	Q385	2070	12.67	1240	260	67.2
LCL	Q399	2145	12.66	1260	260	67.2
Discovery Deep						
Trans	N22	1910	8.66	11.0	40.6	22.3
Trans	N23	1917	8.37	10.4	40.6	23
Trans	N24	1938	9.91	17.1	41	23.7
Trans	N25	1960	10.2	23.2	43	24.5
Trans	N27	1995	11.2	29.1	44	25.1
Trans	N28	2010	11.6	74	50	26.2
Trans	N29	2020	12.0	123	61	27.8
Trans	N30	2030	12.3	325	97	31.6
LCL	N32	2060	12.1	1070	260	45
LCL	N31	2085	12.2	1230	260	45
LCL	Q357	2085	12.7	1210	260	45
Kebrit Deep						
WC	N40	1370	1.66	3.94	40.6	21.6
WC	N41	1381	1.65	3.85	40.6	21.6
WC	N42	1424	1.69	3.89	40.6	21.6
WC	Q417	1424	1.62	3.80	40.6	21.6
WC	N43	1440	1.64	3.86	40.6	21.6
WC	N44	1465	1.63	3.88	40.6	21.7
Trans	Q80	1467	1.53	4.71	42	21.9
LCL	Q200	1534	1.06	57.3	260	23.5
RSDW			1.66	3.9	40.6	21.6

N denotes Niskin samples, Q denotes in situ samples. The measured helium concentrations are reported as cm^3 STP per g RSDW in order to correct for the large salinity variation between the individual brine layers and RSDW. The accuracy of the helium concentrations and $^3He/^4He$ ratios is better than ±1% [24,25]. Note that the noble gas concentrations in the lowest brine layer (LCL) are depleted by 25–30% due to sub-seafloor boiling. However, this boiling process and loss of noble gases does not affect any of the implications or the conclusions drawn here as neither isotope nor elemental fractionation occurs as has been shown in our recent work on the atmospheric noble gases [16].

[a]Temperature and salinity data are from [9,44].

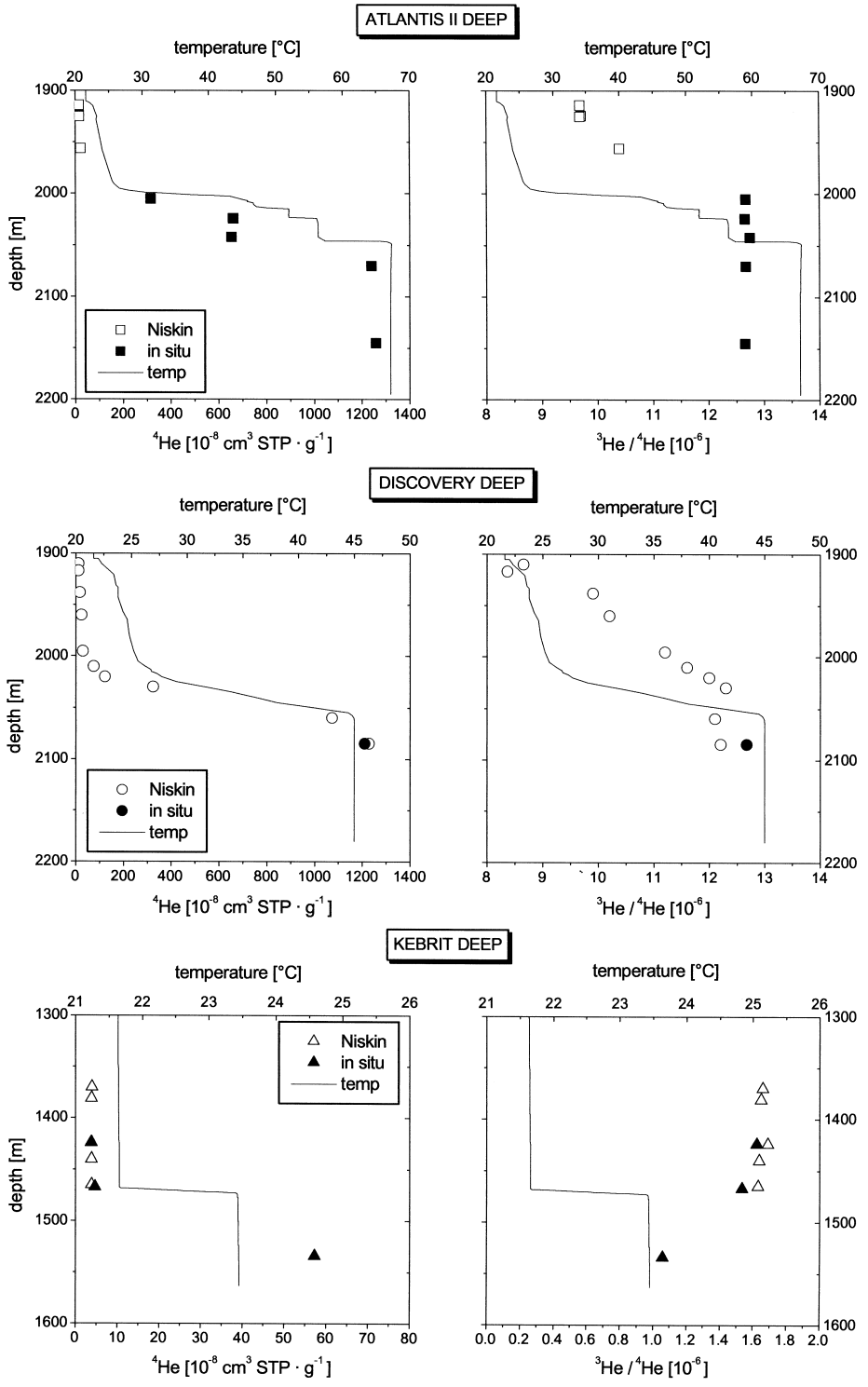

Fig. 2. Vertical profiles showing temperature and ^{4}He (left column) and ^{3}He/^{4}He (right column) in the Atlantis II, Discovery and Kebrit deeps. Solid symbols indicate samples taken with the in situ sampler, open symbols indicate Niskin bottle samples.

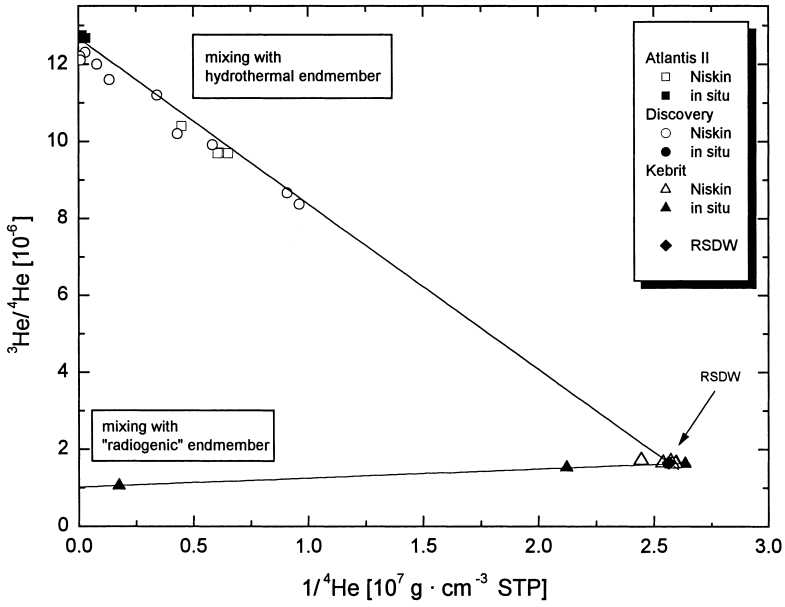

Fig. 3. Correlation of the $^3He/^4He$ ratio with the reciprocal ^4He concentration ($1/^4He$). Solid symbols indicate in situ samples, open symbols indicate Niskin samples. Different symbols represent the three different deeps (square = Atlantis, circle = Discovery, triangle = Kebrit). The samples from the Atlantis and the Discovery deeps define a mixing line between RSDW and a hydrothermal endmember represented by the in situ samples from the Atlantis II system. The helium isotope ratio of this source (1.27×10^{-5} ($9.2\times R_a$)) is given by the intercept with the y-axis. The samples from the Kebrit brine show a completely different behavior. The conventional samples plot near the point for RSDW. The in situ samples from the Kebrit Deep lie on a mixing line between RSDW and a ^4He-enriched radiogenic endmember with a $^3He/^4He$ ratio of 1×10^{-6}.

12 Niskin samples and one in situ sample in the LCL (Q357, duplicate of N31, see Table 1). In both basins, the ^4He concentrations as well as the $^3He/^4He$ ratios increase with depth. Maximum helium excesses are found in the deepest brine layer, the LCL, with ^4He concentrations of about 1.26×10^{-5} cm^3 STP g^{-1} and maximum ^3He concentrations of 1.59×10^{-10} cm^3 STP g^{-1} reflecting an enrichment by up to a factor of 2500 compared to Red Sea Deep Water (RSDW).

The in situ samples from the Atlantis II and Discovery deeps were additionally analyzed for the heavier noble gases [16] and show significantly enhanced $^{40}Ar/^{36}Ar$ ratios (Table 2) of up to 305 compared to 295.5 for atmospheric argon.

3.2. Kebrit Deep

The Kebrit Deep is characterized by a single brine layer with the upper boundary at 1465 m water depth. It differs from the Atlantis II Deep system in some of its geochemical and hydrographic characteristics. Although the salinity of the brine (260‰) is similar to that of the Atlantis II Deep, the Kebrit brine shows only a slight temperature anomaly of +1.9°C compared to the RSDW temperature of 21.6°C. The transition zone between the brine layer (LCL) and RSDW is much sharper than in the Discovery and Atlantis II deeps. We obtained six Niskin samples from above the interface which do not show any significant deviation from RSDW and three in situ samples (see Table 1), Q200 inside the LCL, Q80 from the interface and Q417 from the water column above the brine body. The ^4He concentration of the in situ samples increases with depth but to a much smaller extent than in the other basins (Table 1 and Fig. 2). The ^4He concentration of in situ sample Q200 within the Kebrit brine is 5.7×10^{-7} cm^3 STP g^{-1} reflecting a 15-fold enrichment compared to RSDW. In strong contrast to the Atlantis II and the Discovery

deeps, $^3He/^4He$ ratios decrease with depth to a value of 1.06×10^{-6} within the brine layer, which is significantly lower than the RSDW value.

4. Discussion

In all deeps, significant helium excesses were detected. However, we identified principal differences between the Atlantis II/Discovery deeps and the Kebrit Deep. The geochemical processes responsible for the different helium isotope signatures are discussed in the following sections.

4.1. Atlantis II and Discovery deeps

In Fig. 3, the $^3He/^4He$ ratio is plotted as a function of the reciprocal ^4He concentration. All data from the Atlantis II and the Discovery deep fall on a two-component mixing line between RSDW and a helium-rich endmember. The $^3He/^4He$ ratio of the helium excess endmember is 1.27×10^{-5} ($9.2\times R_a$) as given by the intercept with the y-axis implying the helium excess to be of mantle origin. The observed $^3He/^4He$ ratio is close to that of local submarine basalts from the Atlantis II area reported by Moreira et al. [27]. It is slightly higher than typical values for MORB ($7–9\times R_a$ [28]) reflecting a small contribution of a ^3He-enriched plume component (probably the Afar hotspot) [27].

Prior to our study, there has been only one investigation of the helium isotope characteristics of the Red Sea brines [12]. The helium concentration of the LCL in the Atlantis II Deep in 1966 was found to be 1.34×10^{-5} cm^3 STP g^{-1} with a $^3He/^4He$ ratio of 1.2×10^{-5}. Within the limits of their accuracy, these results agree with our helium data. The correspondence implies that apparently the helium excess has remained stable over the last 30 years reflecting steady-state conditions. This is of major interest particularly with respect to hydrographic investigations proving the Atlantis II Deep to be a highly dynamic system over the last three decades, e.g. warming of the LCL from 55.9°C in 1964 to 67.2°C in 1997 and formation of new layers [9,10]. However, lack of data, in particular of the helium concentration of the

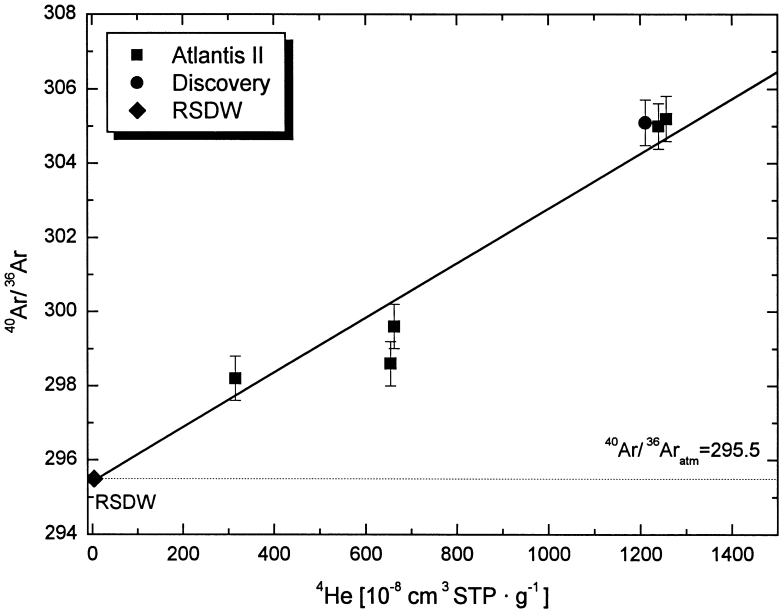

Fig. 4. Correlation of the $^{40}Ar/^{36}Ar$ ratio with the ^4He concentration for the in situ samples from the Atlantis II and Discovery deeps. The positive correlation between $^{40}Ar/^{36}Ar$ and the mantle-derived helium component suggests that mantle-derived ^{40}Ar is transported along with the mantle helium in the brine fluid.

UCL in 1966, prevents further quantitative balance considerations.

The $^{40}Ar/^{36}Ar$ ratio of the in situ samples is correlated to the ^{4}He excess (Fig. 4). In contrast to an early study of the argon concentration [29] we did not observe significant differences of the LCL argon signature between the Atlantis II and Discovery brines (Table 2). The $^{40}Ar/^{36}Ar$ ratio of the LCL in both brines is 305 corresponding to a ^{40}Ar excess of about 3% relative to the atmospheric argon concentration. In situ production of the ^{40}Ar excess in the brine ($[K] = 0.18$ [13]) or the sediments ($[K] = 1.3\%$ [8]) requires accumulation times of the order of millions of years, a possibility highly unlikely for an active hydrothermal system.

The brine samples have a small range in their ^{4}He to ^{40}Ar excess ratio, between 1.5 and 2.7 (Table 2) with a mean value of 2.1. These values fall within the range of current theoretical production ratios of 1.8–4 in the upper mantle as estimated from U, Th and K contents and mantle degassing models [30,31].

As suggested by the positive correlation shown in Fig. 4 and the $(^{4}He/^{40}Ar)_{excess}$ ratio, we conclude that the excess ^{40}Ar, like the helium component, is derived from a mantle source. The correspondence between the measured and the theoretical $(^{4}He/^{40}Ar)_{excess}$ implies that the argon component is derived from a newly injected fresh basaltic source that has not undergone significant outgassing. Up to now, argon isotope anomalies could only be detected in very few marine hydrothermal systems, i.e. in high-temperature vent fluids [22] and in hydrothermal fluid inclusions [23] at the East Pacific Rise. Our study adds further evidence that mantle-derived argon is transported in hydrothermal fluids along with mantle-derived helium at active seafloor hydrothermal systems.

4.2. Kebrit Deep

The situation in the Kebrit Deep appears to be fundamentally different from the situation in the Atlantis II and Discovery deeps. We base our discussion on the in situ samples which are marked with a solid triangle in Fig. 3. The isotope signature of the two samples from the interface and the Kebrit brine itself can be interpreted in terms of a two-component mixture between RSDW and a ^{4}He-enriched endmember. The $^{3}He/^{4}He$ ratio of this endmember is 1×10^{-6} as interpreted from the intercept of the mixing line with the y-axis. As this $^{3}He/^{4}He$ ratio is significantly lower than the atmospheric ratio ($R_a = 1.384\times10^{-6}$), it points to a ^{4}He-rich source of the helium excess. The only plausible source for such a predominantly radiogenic helium excess is the diffusive helium flux of deep crustal or sedimentary origin that is globally observed and is

Table 2
Argon isotope data of the in situ samples from the Atlantis II and Discovery Deep

Sample	Layer	Depth (m)	^{4}He (10^{-8} cm^3 STP g^{-1} RSDW)	$^{40}Ar/^{36}Ar$	$^{40}Ar_{total}$ (10^{-4} cm^3 STP g^{-1} RSDW)	$^{40}Ar_{excess}$ (10^{-6} cm^3 STP g^{-1} RSDW)	$(^{4}He/^{40}Ar)_{excess}$
RSDW			3.9	295.5	2.32	0	
Atlantis II Deep							
Q407	UCL3	2005	315	298.2	2.30	2.1	1.5
Q261	UCL1	2024	626	299.6	2.23	3.1	2.0
Q67	UCL1	2042	655	298.6	2.35	2.4	2.7
Q385	LCL	2070	1240	305	1.85	5.8	2.1
Q399	LCL	2145	1260	305.2	1.91	6.1	2.1
Discovery Deep							
Q357	LCL	2085	1210	305.1	1.87	5.9	2.1

The precision of the measurements of the He and Ar concentrations is better than ±1%, for the isotopic ratio $^{40}Ar/^{36}Ar$ the precision is 0.2% [25]. Excess ^{40}Ar concentrations were calculated from $^{40}Ar_{excess} = {}^{40}Ar_{total}[1-(^{40}Ar/^{36}Ar)_{atm}/(^{40}Ar/^{36}Ar)_{meas}]$ with $(^{40}Ar/^{36}Ar)_{atm} = 295.5$.

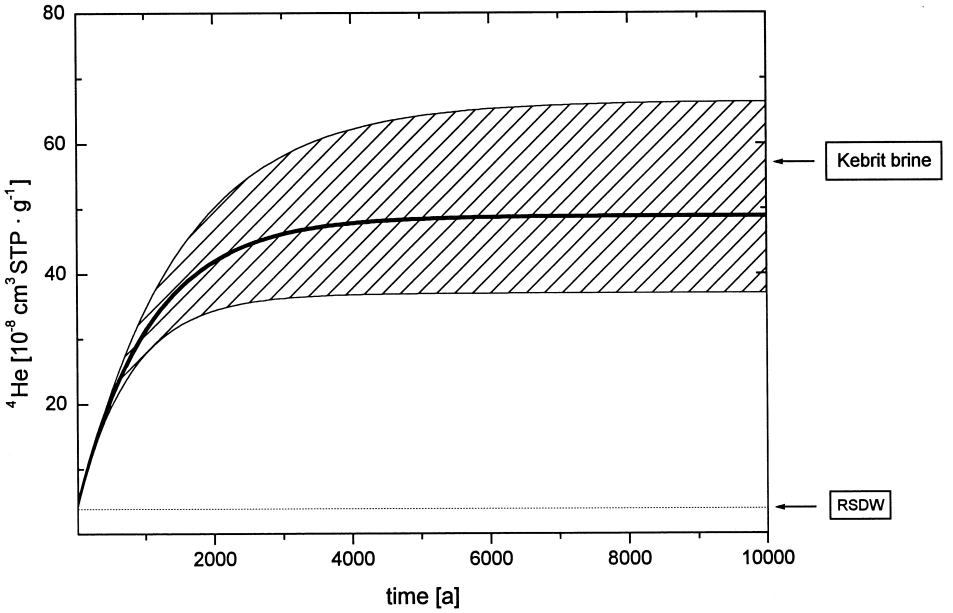

Fig. 5. Temporal evolution of the ^{4}He concentration in the Kebrit brine derived from the accumulation scenario: helium is transported by the diffusive flux from the deep sediment (or crust) and progressively accumulated in the Kebrit brine. The solid line gives the results of the calculation for a helium diffusion coefficient of 4.6×10^{-5} cm^2 s^{-1} and an interface thickness of 2.5 m. The interface thickness (2.5 ± 0.3 m) was derived from the sound velocity profile [44], which reflects the salinity profile and is representative of the transport of dissolved gases. The diffusion coefficient was obtained by linear extrapolation of the data for pure and seawater [45] as the diffusivity of a solute in an aqueous electrolyte is known to decrease approximately linearly with the concentration of the electrolyte [46]. The extrapolation yields a diffusion coefficient of $D_{He}=(4.6\pm0.9)\times10^{-5}$ cm^2 s^{-1}, approximately 35% lower than the diffusion coefficient for seawater (7×10^{-5} cm^2 s^{-1}). The shaded area represents the maximum and minimum model outputs obtained by variation of the model parameters D_{He} and z within their uncertainties given in the parentheses.

conceptually explained by continuous helium production by α-decays of the ubiquitous U- and Th-series elements in the entire crust (e.g. [32–34]).

The low isotope ratio of the helium excess allows us to exclude active hydrothermal mantle-derived fluid input as a major source of the Kebrit brine as in the case of the Atlantis II Deep. Instead, we propose a diffusive flux scenario: after formation of the brine, probably through surface dissolution of outcropping evaporites by overlying seawater as proposed earlier for the Valdivia brine [13], helium from deep sedimentary or crustal strata migrates upward into the brine where it is subsequently accumulated due to the stratification and isolation of the brine from the overlying water column.

Additional evidence for a diffusive flux scenario comes from the hydrocarbon data. The Kebrit brine shows very high methane concentrations of up to 22 ml l^{-1} [26]. Its isotopic signature is thermogenic [26] suggesting that the methane is produced in the deeper sediments by thermal degradation and then – as the crustal helium – migrates upward into the deep.

4.2.1. *The diffusive flux scenario*

To evaluate the flux hypothesis, we simulate the accumulation process with a simplified one-dimensional model considering the two essential transport processes: the helium flux entering the brine from the sediment and the exchange at the brine–seawater interface. Assuming the brine to be well mixed by convection as indicated by the homogeneous temperature distribution (Fig. 2), the change in the helium concentration of the

brine with time, t, is described by:

$$\frac{\partial C}{\partial t} = \frac{J_{\text{crust}}}{h\rho} - \frac{D_{\text{He}}}{zh}\{C(t) - C_0\} \quad (1)$$

The first term on the right-hand side of the equation denotes the contribution by the constant crustal flux J_{crust} which is chosen to be the value for average continental crust ($J_{\text{crust}} = 3.1 \times 10^{-6}$ cm^3 STP cm^{-2} yr^{-1} [35]) since the Kebrit Deep is assumed to be underlaid by continental crust [3]. The second term denotes the diffusive loss at the interface according to Fick's law. Because of the steep salinity gradient advective transport and turbulent exchange can be ignored and the transport process across the brine–seawater interface is mainly controlled by molecular diffusion (e.g. [11]). Here, h is the average vertical extension of the brine (62 m), D_{He} is the molecular diffusion coefficient (4.6×10^{-5} cm^2 s^{-1}), ρ is the density of the brine (1.19 g cm^{-3}), z is the interface thickness (2.5 m) and C_0 is the helium concentration of RSDW (3.9×10^{-8} cm^3 STP g^{-1}, see Table 1).

Under the boundary condition that the helium concentration at $t = 0$ is the RSDW concentration ($C_{|t=0} = C_0$), the differential equation can be solved analytically:

$$C(t) = C_0 + \frac{J_{\text{crust}} z}{\rho D_{\text{He}}}\left\{1 - \exp\left(-\frac{D_{\text{He}} t}{zh}\right)\right\} \quad (2)$$

Fig. 5 shows the temporal evolution of the ^{4}He concentration of the brine as derived from the model. After several thousand years, the steady state between input and loss is reached, and the helium concentration does not continue to increase. The steady-state helium concentration of the brine according to the model is 4.9×10^{-7} cm^3 STP g^{-1}, the conservative range obtained by variation of the input parameters is between 3.7×10^{-7} and 6.6×10^{-7} cm^3 STP g^{-1} (see caption of Fig. 5).

The measured concentration of the Kebrit brine of 5.7×10^{-7} cm^3 STP g^{-1} is in excellent agreement with this model, particularly when considering the simplicity of the concept. Obviously, the input of an average crustal helium flux from the sediment can plausibly explain the helium concentration measured in the Kebrit brine. Furthermore, the model gives an estimate of the time period needed to accumulate the observed helium concentration and thus, a minimum residence time of the brine of the order of a thousand years.

The hypothesis of steady-state conditions of the Kebrit brine may be tested by considering the temperature distribution: if the assumption of steady state holds, the input of heat from the bottom of the Deep must be balanced by the vertical transport of heat across the brine–water column interface [11,36]. The diffusive heat flux through the interface is given by:

$$F_{\text{heat}} = \rho c_{\text{p}} K_{\text{th}} \frac{\Delta T}{\Delta z} \quad (3)$$

where K_{th} is the thermal diffusivity, ρ the density, c_{p} the heat capacity and $\Delta T/\Delta z$ the vertical gradient of heat across the interface (0.475°C m^{-1}, Fig. 2). Again, the dominant mechanism of heat transport is molecular heat diffusion ($K_{\text{th}} = 1.52 \times 10^{-3}$ cm^2 s^{-1} [37]). The numerical value of the heat capacity c_{p} (3.180 J g^{-1} K^{-1}) was calculated for the temperature and salinity of the brine using data for NaCl aqueous solution [38].

From Eq. 3 we obtain a heat flux of 273 mW m^{-2}. This value is consistent with heat flow data of 200–300 mW m^{-2} that has been measured in the axial zone of the northern Red Sea close to the location of the Kebrit Deep [39]. The correspondence implies that the heat loss at the upper interface is compensated by the geothermal heat flux and that there is no advective hydrothermal heat input. This gives further evidence that the Kebrit brine is in a steady state with respect to both the geothermal heat flow and the diffusive crustal helium flux.

The diffusive flux model presented here might be used as a plausible scenario for other systems as well. The Discovery Basin, a deep brine basin in the eastern Mediterranean, shows a radiogenic helium excess of 6×10^{-7} cm^3 STP g^{-1} [40], very similar to the helium concentration of the Kebrit brine. Likely, this helium excess is also related to a crustal diffusive helium flux which accumulates in the brine.

4.3. Isotopic signatures and geological setting

The Atlantis II and Kebrit brines show distinct isotopic characteristics that reflect their different geological settings, i.e. the transition from a continental to an oceanic rift system.

The Kebrit brine located in the northern part of the Red Sea shows a predominantly radiogenic helium signature which is interpreted as the result of a continental crustal flux accumulating in the brine. This is consistent with the geological setting of the northern part of the Red Sea where the continental crust is stretched and thinned representing pre-seafloor spreading conditions [4]. The extensional character is reflected in our helium isotope data in that the Kebrit brine has a $^3He/^4He$ ratio significantly exceeding the average radiogenic production ratio for crustal helium ($1–3\times10^{-8}$). Thus it represents a mixture of a pure radiogenic component ($0.02R_a$) and a mantle contribution ($9R_a$). Simple isotope balance calculations yield that a fraction of 9% of the helium present in the Kebrit brine is mantle-derived and required to explain the enhanced $^3He/^4He$ ratio relative to pure radiogenic production. In other words, the crustal helium flux carries a mantle component of approximately 9%. The mantle helium component probably originates from intrusions of mantle material accompanying the crustal extension. Thus, the enhanced $^3He/^4He$ ratio can be interpreted as a sensitive indicator of a mantle involvement in crustal processes as has been found earlier in relatively unstable continental areas (e.g. [41]).

On the other hand, the Atlantis II and Discovery deeps are located in the middle segment of the Red Sea which is presently changing from diffusive extension to seafloor spreading mode of plate separation [4]. The deeps are interpreted as initiation points, i.e. as the locations where seafloor spreading has recently started. This process is accompanied by active subbottom hydrothermal circulation with hydrothermal discharge that carries the mantle-derived helium and argon signatures.

5. Conclusions

Our study reveals significant differences of helium and argon isotope data along the Red Sea rift system. The geochemical findings are in striking agreement with the northward progression of seafloor spreading in the Red Sea. (i) In the southern Atlantis II and Discovery brines, helium and argon signatures, and particularly the $(^4He/^{40}Ar)_{excess}$, are MORB-like implying association with an active hydrothermal circulation system. Our study proves the high potential of combining helium and argon isotope studies of fluids to determine crucial parameters for geochemical mantle processes. (ii) In contrast, the Kebrit Deep in the northern Red Sea has a low $^3He/^4He$ signature indicating a predominantly crustal origin and no signs of active hydrothermal input. The Kebrit signature can be explained by a diffusive crustal helium flux entering the deep from below. These findings suggest a new interpretation of the formation of the Kebrit brine system which is not in accordance with the conclusions drawn by [42,43] who attribute the Kebrit brine to hydrothermal fluids passing through sedimentary package prior to discharge similar to the hydrothermal system of the Guaymas Basin. The scenario suggested for the Kebrit brine may possibly apply to other marine systems.

Acknowledgements

Mark Schmidt provided support at sea during cruise SO-121 and helpful discussion of our preliminary results. Steffen Schuler is thanked for his assistance with the helium isotope analyses at the University of Heidelberg. The manuscript benefited from constructive reviews by David Hilton and Peter Schlosser. *[EB]*

References

[1] J.R. Cochran, A model for the development of the Red Sea, Am. Assoc. Petrol. Geol. 67 (1983) 41–69.
[2] E. Bonatti, P. Colantoni, B. Della Vedova, M. Taviani, Geology of the Red Sea transitional region (22°N–25°N), Ocean. Acta 7 (1984) 385–398.

[3] J.R. Cochran, F. Martínez, M.S. Steckler, M.A. Hobart, Conrad Deep: a new northern Red Sea deep. Origin and implications for continental rifting, Earth Planet. Sci. Lett. 78 (1986) 18–32.
[4] E. Bonatti, Punctiform initiation of seafloor spreading in the Red Sea during transition from a continental to an oceanic rift, Nature 316 (1985) 33–37.
[5] E.T. Degens, D.A. Ross, Hot Brines and Recent Heavy Metal Deposits in the Red Sea, Springer-Verlag, Berlin, 1969, 600 pp.
[6] H. Bäcker, M. Schoell, New deeps with brines and metalliferous sediments in the Red Sea, Nature (Phys. Sci.) 240 (1972) 153–158.
[7] G. Pautot, P. Guennoc, A. Coutelle, N. Lyberis, Discovery of a large brine deep in the northern Red Sea, Nature 310 (1984) 133–136.
[8] F.T. Manheim, Red Sea geochemistry, in: R.B. Whitmarsh, O.E. Weser, D.A. Ross (Eds.), Initial Reports of the Deep Sea Drilling Project, Vol. 23, US Government Printing Office, Washington, DC, 1974, pp. 975–998.
[9] M. Hartmann, J.C. Scholten, P. Stoffers, F. Wehner, Hydrographic structure of brine-filled deeps in the Red Sea: new results from the Shaban, Kebrit, Atlantis II and Discovery Deep, Mar. Geol. 144 (1998) 311–330.
[10] P. Anschutz, J.S. Turner, G. Blanc, The development of layering, fluxes through double-diffusive interfaces, and location of hydrothermal sources of brines in the Atlantis II Deep: Red Sea, J. Geophys. Res. 103 (C12) (1998) 27809–27819.
[11] P. Anschutz, G. Blanc, F. Chatin, M. Geiller, M.-C. Pierret, Hydrographic changes during 20 years in the brine-filled basins of the Red Sea, Deep-Sea Res. 46 (1999) 1779–1792.
[12] J.E. Lupton, R.F. Weiss, H. Craig, Mantle helium in the Red Sea brines, Nature 266 (1977) 244–246.
[13] R.A. Zierenberg, W.C. Shanks III, Isotopic constraints on the origin of the Atlantis II, Suakin and Valdivia brines, Red Sea, Geochim. Cosmochim. Acta 50 (1986) 2205–2214.
[14] G. Blanc, J. Boulègue, A. Michard, Isotope composition of the Red Sea hydrothermal endmember, C.R. Acad. Sci. Paris 320 (1995) 1187–1193.
[15] P. Anschutz, G. Blanc, P. Stille, Origin of fluids and the evolution of the Atlantis II deep hydrothermal system, Red Sea: Strontium isotope study, Geochim. Cosmochim. Acta 59 (1995) 4799–4808.
[16] G. Winckler, R. Kipfer, W. Aeschbach-Hertig, R. Botz, M. Schmidt, S. Schuler, R. Bayer, Sub sea floor boiling of Red Sea brines: New indication from noble gas data, Geochim. Cosmochim. Acta 64 (9) (2000) 1567–1575.
[17] W.B. Clarke, W.J. Jenkins, Z. Top, Determination of tritium by mass spectrometric measurement of ^{3}He, Int. J. Appl. Rad. Isot. 27 (1976) 515–522.
[18] B.A. Mamyrin, I.N. Tolstikhin, Helium Isotopes in Nature, Elsevier, Amsterdam, 1984, 273 pp.
[19] J.E. Lupton, Terrestrial inert gases: Isotope tracer studies and clues to primordial components in the mantle, Annu. Rev. Earth Planet. Sci. 11 (1983) 371–414.
[20] T. Staudacher, P. Sarda, S.H. Richardson, C.J. Allègre, I. Sagna, L.V. Dimitriev, Noble gases in basalt glasses from a Mid-Atlantic ridge topographic high at 14°N: geodynamic consequences, Earth Planet. Sci. Lett. 96 (1989) 119–133.
[21] D.A. Butterfield, G.J. Massoth, R.E. McDuff, J.E. Lupton, M.D. Lilley, Geochemistry of hydrothermal fluids from Ashes Vent Field, Axial Seamount, Juan de Fuca Ridge: Subseafloor boiling and subsequent fluid-rock interaction, J. Geophys. Res. 95 (B8) (1990) 12895–12921.
[22] M. Bender, J. Orchardo, M. Lilley, J. Lupton, K. Von Damm, J. Edmond, ^{40}Ar outgassing from the mantle reflected in the ^{36}Ar/^{40}Ar ratio of hydrothermal vent fluids from the East Pacific Rise, 9°N, EOS 72 (1991) 481.
[23] F.M. Stuart, G. Turner, Mantle-derived ^{40}Ar in mid-ocean ridge hydrothermal fluids: implications for the source of volatiles and mantle degassing rates, Chem. Geol. 147 (1998) 77–88.
[24] R. Bayer, P. Schlosser, G. Bönisch, H. Rupp, F. Zaucker, G. Zimmek, Performance and blank components of a mass spectrometric system for routine measurement of helium isotopes and tritium by the ^{3}He ingrowth method, Sitzungsber. Heidelberger Akad. Wissensch. 5 (1989) 241–279.
[25] U. Beyerle, W. Aeschbach-Hertig, D.M. Imboden, H. Baur, T. Graf, R. Kipfer, A mass spectrometric system for the analysis of noble gases and tritium from water samples, Environ. Sci. Technol. (2000) (in press).
[26] E. Faber, R. Botz, J. Poggenburg, M. Schmidt, P. Stoffers, M. Hartmann, Methane in Red Sea brines, Org. Geochem. 29 (1998) 363–379.
[27] M. Moreira, P.J. Valbracht, T. Staudacher, C.J. Allègre, Rare gas systematics in Red Sea ridge basalts, Geophys. Res. Lett. 23 (1996) 2453–2456.
[28] K.A. Farley, E. Neroda, Noble gases in the earth's mantle, Annu. Rev. Earth Planet. Sci. 26 (1998) 189–218.
[29] R.F. Weiss, Dissolved argon, nitrogen and total carbonate in the Red Sea brines, in: E.T. Degens, D.A. Ross (Eds.), Hot Brines and Recent Heavy Metal Deposits in the Red Sea, Springer, New York, 1969, pp. 254–260.
[30] C.J. Allègre, T. Staudacher, P. Sarda, Rare gas systematics: formation of the atmosphere, evolution and structure of the Earth's mantle, Earth Planet. Sci. Lett. 81 (1987) 127–150.
[31] P.G. Burnard, K.A. Farley, G. Turner, Multiple fluid pulses in a Samoan harzburgite, Chem. Geol. 147 (1998) 99–114.
[32] T. Torgersen, W.B. Clarke, Helium accumulation in groundwater. I. An evaluation of sources and the continental flux of crustal ^{4}He in the Great Artesian Basin, Australia, Geochim. Cosmochim. Acta 49 (1985) 1211–1218.
[33] R.K. O'Nions, E.R. Oxburgh, Helium, volatile fluxes and the development of continental crust, Earth Planet. Sci. Lett. 90 (1988) 331–347.

[34] R. Hohmann, M. Hofer, R. Kipfer, F. Peeters, D.M. Imboden, Distribution of helium and tritium in Lake Baikal, J. Geophys. Res. 103 (C6) (1998) 12823–12838.
[35] T. Torgersen, Terrestrial helium degassing fluxes and the atmospheric helium budget: Implications with respect to the degassing processes of the continental crust, Chem. Geol. 79 (1989) 1–14.
[36] W. Aeschbach-Hertig, M. Hofer, R. Kipfer, D.M. Imboden, R. Wieler, Accumulation of mantle gases in a permanently stratified volcanic lake (Lac Pavin, France), Geochim. Cosmochim. Acta 63 (1999) 3357–3372.
[37] Landolt-Börnstein, Zahlenwerte und Funktionen aus Physik, Chemie, Astronomie, Geophysik und Technik, in: K.H. Hellwege (Ed.), II. Band: Eigenschaften der Materie in ihren Materialzuständen – Transportphänomene, Kinetik, Homogene Gasgleichgewichte, Vol. 5b, Springer, Berlin, 1968.
[38] K.S. Pitzer, J.C. Peiper, R.H. Busey, Thermodynamic properties of aqueous sodium chloride solutions, J. Phys. Chem. Ref. Data 13 (1984) 1–102.
[39] F. Martínez, J.R. Cochran, Geothermal measurements in the northern Red Sea: implications for lithospheric thermal structure and mode of extension during continental rifting, J. Geophys. Res. 94 (B9) (1989) 12239–12265.
[40] G. Winckler, E. Suess, K. Wallmann, G.J. De Lange, G.K. Westbrook, R. Bayer, Excess helium and argon of radiogenic origin in Mediterranean brine basins, Earth Planet. Sci. Lett. 151 (1997) 225–231.
[41] R.K. O'Nions, E.R. Oxburgh, Heat and helium in the Earth, Nature 306 (1983) 429–436.
[42] N. Blum, H. Puchelt, Sedimentary-hosted polymetallic massive sulfide deposits of the Kebrit and Shaban Deeps, Red Sea, Min. Deposita 26 (1991) 217–227.
[43] W. Michaelis, A. Jenisch, H.H. Richnow, Hydrothermal petroleum generation in Red Sea sediments from the Kebrit and Shaban Deeps, Appl. Geochem. 5 (1990) 103–114.
[44] P. Stoffers and shipboard party, Cruise Report Sonne 121-Red Sea: Hydrography, hydrothermalism and paleoceanography in the Red Sea, Reports, Geologisch-Paläontologisches Institut und Museum CAU, Kiel, 1998, 107 pp.
[45] B. Jähne, G. Heinz, W. Dietrich, Measurement of the diffusion coefficients of sparingly soluble gases in water, J. Geophys. Res. 92 (1987) 10767–10776.
[46] G.A. Ratcliff, J.G. Holdcroft, Diffusivities of gases in aqueous electrolyte solutions, Trans. Inst. Chem. Eng. 41 (1963) 315–319.